Mechanisms of Evasion to Antiangiogenic Therapy in Glioblastoma

Samuel D. Rose, BS, and Manish K. Aghi, MD, PhD

Recognition of the role of vascular endothelial growth factor (VEGF) in developing the rich vascularity of glioblastomas, which contributes to their growth and resistance to radiation, surgery, and chemotherapy, has led to clinical trials of agents targeting VEGF or VEGF receptors 1 and 2. VEGF has been targeted with the mouse anti-human VEGF antibody avastin (bevacizumab), which has undergone phase II clinical trials in glioma patients.[1,2] VEGF receptors have been targeted in phase II clinical trials in glioma patients using the tyrosine kinase inhibitor AZD2171[3] and the protein kinase C-β inhibitor enzastaurin.[4] Encouraging results in phase II clinical trials studying bevacizumab treatment of recurrent glioblastomas[1,2] led to the May 6, 2009, accelerated Food and Drug Administration (FDA) approval of bevacizumab for recurrent glioblastoma treatment, making bevacizumab just the third FDA-approved treatment for glioblastoma in nearly 4 decades and leading to a Radiation Therapy Oncology Group–sponsored phase III clinical trial that will soon begin in primary glioblastomas comparing radiation and temozolomide, a DNA-damaging agent that is the existing standard of care in glioblastoma chemotherapy, meaning that bevacizumab may soon become part of the standard treatment regimen for both primary and recurrent glioblastomas.

Unfortunately, 43% of recurrent glioblastomas failed to respond to bevacizumab in the phase II clinical trials,[1,2] and despite initial responsiveness, other glioblastomas frequently grow during bevacizumab treatment. Preclinical studies have suggested that, unlike the gene mutations that cause tumor cell resistance to DNA-damaging chemotherapy, tumor cells become resistant to antivascular agents by evasive mechanisms, ie, adaptive nongenetic mechanisms like transcriptional upregulation that allow tumor cells to find alternative ways of sustaining tumor growth while the antivascular target remains inhibited.[5] Evasion to antiangiogenic therapy differs from classic chemotherapy resistance in that these evasive mechanisms reflect transcriptional changes that are generated more readily than the DNA gene mutations that characterize traditional chemotherapy resistance[5]; these responses may occur to some extent in all treated tumors, with only tumors with the greatest transcriptional changes exhibiting tumor growth consistent with evasion to antiangiogenic therapy. At our institution, 15% of patients with recurrent glioblastomas treated with bevacizumab have experienced radiographic progression during treatment after initially responding to bevacizumab, leading to another surgical resection, consistent with acquired bevacizumab evasion. Half of these bevacizumab-evasive glioblastomas (BEGs) have exhibited nonenhancing infiltrative regrowth and half have shown nodular-enhancing regrowth (Figure 1), suggesting the possibility of at least 2 different bevacizumab evasion mechanisms causing glioblastoma regrowth. Unfortunately, regardless of radiographic appearance, BEGs lack any therapeutic option and are invariably rapidly fatal. To identify mediators of these 2 subtypes of bevacizumab evasion, we performed a gene expression analysis and immunohistochemistry comparing BEGs with their paired primary tumors.

METHODS

Case Selection

We retrospectively reviewed 65 recurrent glioblastomas treated with bevacizumab at our institution between September 2005 and October 2007. Cases were reviewed to determine the duration of treatment with bevacizumab, whether the treatment was monotherapy or combined with other agents, the date that bevacizumab was stopped, whether the reason for stopping the drug was finishing a course or radiographic progression, whether the finding of radiographic progression led to surgery or just a change in therapy, and the number of days after the last bevacizumab dose that an operation for radiographic progression occurred. This study was approved by the University of California San Francisco (UCSF) Committee on Human Research.

Immunohistochemistry

Immunohistochemical staining was done on 5-μm formalin-fixed, paraffin-embedded serial tissue sections by incubating overnight at 4°C with primary antibodies to endothelial marker von Willebrand factor (1:200; rabbit polyclonal; Dako,

0148-396X

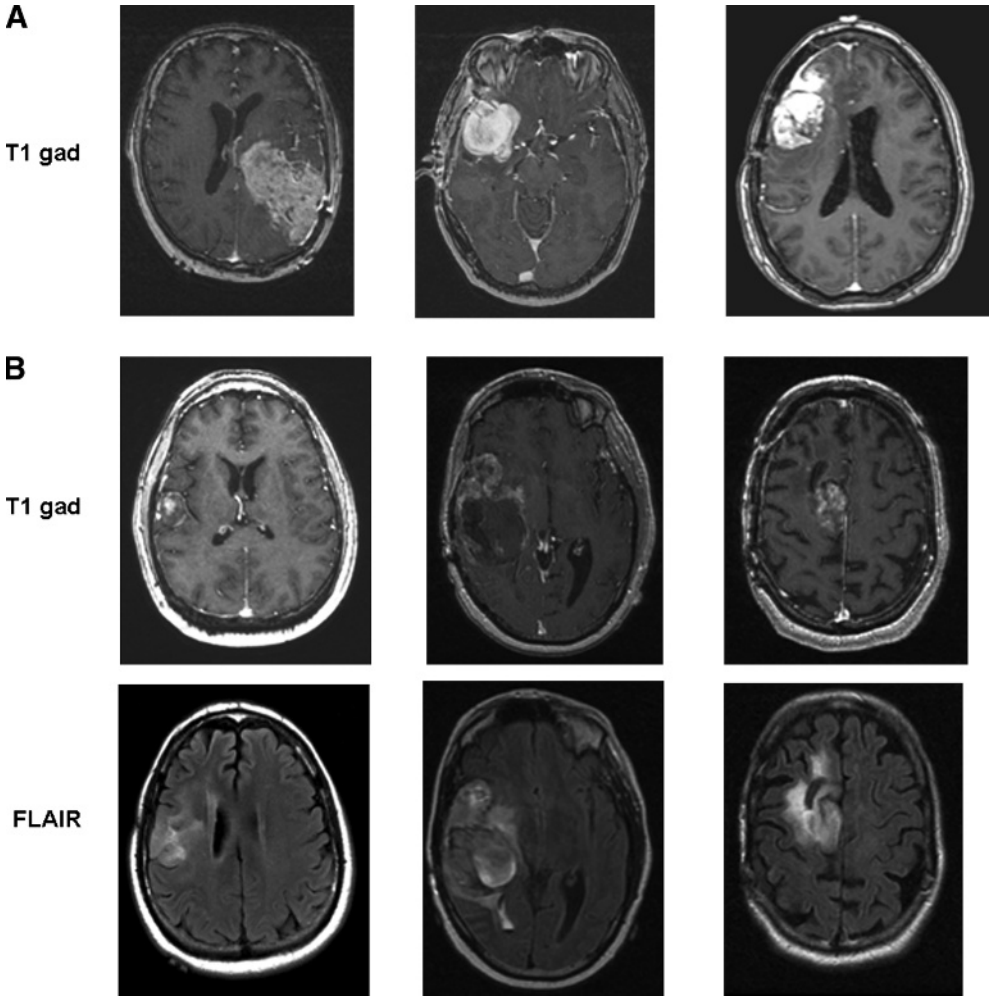

FIGURE 1. Magnetic resonance images of bevacizumab-evasive gliomas (BEGs). A, T1-gadolinium (gad)–enhanced axial images from 3 representative nodular-enhancing BEGs (NEBEGs) are shown. B, T1-gadolinium–enhanced axial images (top row) and FLAIR axial images (bottom row) from 3 representative infiltrating BEGs (IBEGs) are shown.

Glostrup, Denmark), hypoxia marker CA9 (1:1000; rabbit polyclonal; Novus Biologicals, Littleton, Colorado), and c-Met (abcam; Cambridge, Massachusetts), a target identified in the microarray analysis, followed by a 30-minute incubation with a peroxidase-conjugated secondary antibody using the Vector Impress kit (Vector Laboratories, Burlingame, California) and a hematoxylin counterstain. Vesseldensities were counted from 10 representative fields of von Willebrand factor immunostainings by 2 observers blinded to the treatment group. The percentage of tissue that was CA9 positive and the number of c-Met–positive cells were calculated with ImageJ software (National Institutes of Health, Bethesda, Maryland).[6]

Microarray Analysis

RNA was extracted from paraffin blocks with the RecoverAll Total Nucleic Acid Isolation Kit (AM1975; Ambion, Inc, Austin, Texas) using 60 to 120 μm of paraffin sample, depending on the amount of embedded tissue. Concentrations of RNA samples were assessed with a Nanodrop Spectrophotometer, and the quality of the RNA samples was assessed on an Agilent 2100 Bioanalyzer (Agilent Technologies) with the RNA 6000 Nano Kit (Agilent Technologies, Santa Clara, California). Comprehensive microarray transcription analysis was conducted with the DASL Gene Expression Platform (Illumina, Inc, San Diego, California), a microarray platform designed for analysis of formalin-fixed, paraffin-embedded extracted RNA samples. Sample hybridization and microarray chip scanning was conducted in the UCSF Genomics Core Facility, and data were subsequently analyzed in conjunction with a biostatistician in the UCSF Cancer Center. Gene enrichment subset analysis was performed using the molecular signature database C2 gene set collection, which contains 1892 gene sets, with each gene set containing 15 to 500 related genes collected from online pathway databases, publications, and knowledge of domain experts. For individual transcripts, for each of the 25 000 microarray transcripts analyzed on microarrays, raw *P* values were adjusted for multiple testing by controlling the false discovery rate, generating adjusted *P* values.

Matrigel Invasion Assay

Freshly resected BEG tissue was obtained from the operating room and dissociated into single-cell homogenates with the Worthington Papain Dissociation System (Worthington Inc, Lakewood, New Jersey). Red blood cells were lysed for 3 minutes in Pharmlyse Buffer (Becton-Dickinson, Franklin Lakes, New Jersey). Then, 50 000 cells were placed on the top chamber of GFR Matrigel Invasion Chamber Inserts (Becton-Dickinson) in 500 μL serum-free Dulbecco modified Eagle medium and incubated at 37°C in 5% CO_2. In the bottoms of the inserts, 750 μL NIH-3T3–conditioned media was placed as a chemoattractant. Inserts were stained and fixed at various time points ranging from 3 to 48 hours, with cells invading through Matrigel into the bottom of the inserts counted at each time point and measured as a percentage of the number of cells invading from the upper to lower wells in control inserts lacking Matrigel.

Statistical Analyses

Moderated *t* statistics (as implemented in the limma package in R/Bioconductor open source software) were used to test for differentially expressed microarray probes. The theoretical (raw) *P* values were adjusted for multiple testing by controlling the false discovery rate. Immunohistochemistry was analyzed by a paired Student *t* test, with values of $P < .05$ deemed statistically significant.

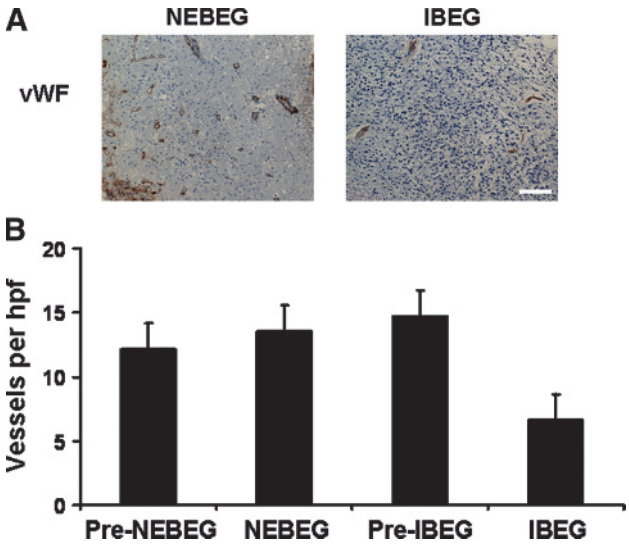

FIGURE 2. von Willebrand factor (vWF) immunostaining of bevacizumab-evasive gliomas (BEGs). A, representative immunostainings of a nodular-enhancing BEG (NEBEG) and an infiltrating BEG (IBEG) are shown. B, the average vessel densities of gliomas before bevacizumab treatment that would go on to become NEBEGs (pre-NEBEGs), NEBEGs, gliomas before bevacizumab treatment that would go on to become IBEGs (pre-IBEGs), and IBEGs are shown, along with standard deviations. Magnification × 100. Scale bar represents 200 μm. hpf, high-powered field.

RESULTS

Of 65 bevacizumab-treated recurrent glioblastomas at our institution between September 2005 and October 2007, 10 developed radiographic progression during treatment, requiring surgery an average of 31 days after their last bevacizumab dose (range, 15-49 days). On their magnetic resonance images (MRIs) showing radiographic progression during bevacizumab treatment, half of these glioblastomas were minimally enhancing fluid-attenuated inversion recovery (FLAIR) bright infiltrative BEGs (IBEGs), and the other half were nodular-enhancing BEGs (NEBEGs) (Figure 1).

Immunohistochemical analyses revealed that IBEGs had 47% of the vessel densities ($P = .04$) and a > 3-fold increase in the percentage of tissue staining positive for the hypoxia-upregulated gene carbonic anhydrase 9 (CA9)[7] ($P = .03$), which correlates with hypoxia, compared with their pre-bevacizumab-treated paired gliomas. On the other hand, NEBEGs had nearly the same vessel densities ($P = .9$) and no change in the percentage of tissue staining for CA9 ($P = .9$) compared with their paired pre-bevacizumab-treated gliomas (Figures 2 and 3).

Microarray analysis was used to compare patients' pre-bevacizumab-treated gliomas and BEGs. Cluster dendograms (not shown) revealed clustering of NEBEGs separately from IBEGs. A gene-enrichment subset analysis revealed that IBEGs exhibited increased expression of gene subsets associated with wound healing, whereas NEBEGs exhibited increased expression of gene subsets associated with vascular injury (Table 1). In terms of individual transcripts, raw *P* values of 25 000 microarray transcripts were adjusted for multiple testing by controlling false discovery rates. Although no transcripts exhibited adjusted $P < .05$, several oncologically pertinent transcripts had raw values of $P = .001$ to .04 and after normalization a > 1.8-fold change in BEGs compared with these patients' primary gliomas (Table 2).

Immunohistochemistry confirmed that IBEGs had elevated expression of c-Met, one of the most differentially expressed factors in IBEGs, compared with their pre–bevacizumab-treated paired gliomas ($P = .009$), whereas NEBEGs had reduced expression of c-Met compared with their pre–bevacizumab-treated paired gliomas in a manner that was barely statistically significant ($P = .05$; Figure 4). We also used Matrigel chambers to measure the invasiveness of cells prospectively obtained from an IBEG and from an NEBEG, and found nearly 3 times more invasiveness in the IBEG compared with the NEBEG ($P = .04$; Figure 5).

DISCUSSION

The average survival of patients with glioblastoma is poor at 12 to 15 months after diagnosis and has unfortunately remained unchanged over the past decade. This lack of

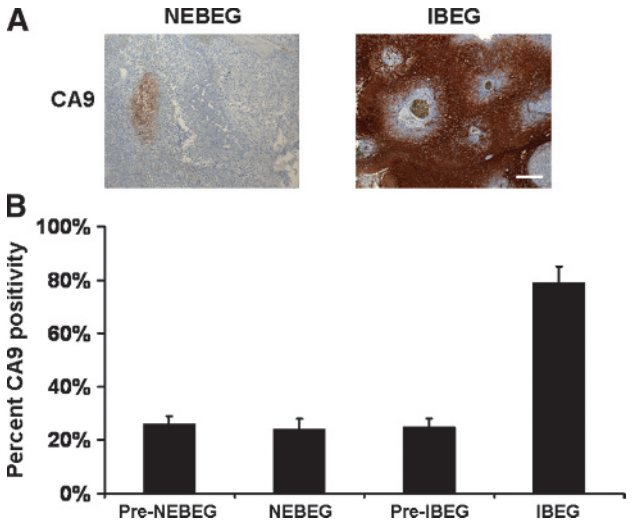

FIGURE 3. Carbonic anhydrase 9 (CA9) immunostaining of bevacizumab-evasive gliomas (BEGs). A, representative CA9 immunostainings of a nodular-enhancing BEG (NEBEG) and an infiltrating BEG (IBEG) are shown. B, the average percentage CA9 positivity of gliomas before bevacizumab treatment that would go on to become NEBEGs (pre-NEBEGs), NEBEGs, gliomas before bevacizumab treatment that would go on to become IBEGs (pre-IBEGs), and IBEGs are shown, along with standard deviations. Magnification × 100. Scale bar represents 200 μm.

progress underscores the importance of understanding unique features of glioblastoma biology and designing novel therapies targeting these unique features. One unique feature of glioblastoma biology is their elevated vessel density, far greater relative to surrounding normal tissue than other tumors. These blood vessels found in glioblastomas are abnormal in appearance in that they are tortuous and disorganized. Glioblastoma blood vessels are also abnormal biologically in that they are highly permeable with abnormal basement membranes, a cause of treatment resistance, and they exhibit endothelial proliferation, a histologically defining feature of glioblastoma. Because VEGF expression allows glioblastomas to acquire much of their abnormal vasculature, clinical trials using the VEGF-neutralizing antibody bevacizumab have been carried out to reduce the number of glioma blood vessels. Encouraging results in phase II clinical trials of bevacizumab for recurrent glioblastoma treatment led to the May 2009 FDA approval of bevacizumab in recurrent glioblastoma treatment, which made bevacizumab only the third FDA-approved chemotherapy for glioblastoma in the past 35 years, along with implantable Gliadel wafers and temozolomide. Unfortunately, like previous DNA-damaging chemotherapies, antiangiogenic therapies like bevacizumab can have brief efficacy, often followed by the development of tumor growth. This loss of response is called evasion in the case of antiangiogenic therapy, to contrast the adaptive, nongenetic transcriptional upregulation seen after antiangiogenic therapy to the DNA mutations that causes resistance to DNA-damaging chemotherapy.

We analyzed a number of glioblastomas that acquired bevacizumab evasion and found that they can be grouped into 2 subtypes. The first type had an infiltrative FLAIR bright appearance on MRI and minimal gadolinium uptake at recurrence. We called them IBEGs. The second type had an enhancing nodular appearance on MRI, and we called them

TABLE 1. Results of Gene-Enrichment Subset Analysis in Bevacizumab-Evasive Gliomas[a]

BEG Subset	Direction of Change	Gene Subset	Change	*P*
NEBEGs	Upregulation	ROS_MOUSE_AORTA_UP (upregulated in mouse aorta treated to mimic hypertension and stimulate vascular dysfunction)	1.9-fold	.01
	Downregulation	RHOPATHWAY (RhoA is a G protein that stabilizes actin and phosphorylates myosin, promoting invasion)	1.5-fold	.03
		ST_INTEGRIN_SIGNALING_PATHWAY (integrins binding extracellular matrix)	1.6-fold	.004
IBEGs	Upregulation	CHANG_SERUM_RESPONSE_DN (upregulated in fibroblasts exposed to serum to model wound healing and in many infiltrative tumors)	1.8-fold	.04
		SERUM-FIBROBLAST_CELLCYCLE (upregulated in fibroblasts after serum exposure, a wound healing model)	2.4-fold	.0004
		SERUM_FIBROBLAST_CORE_UP (upregulated in fibroblast cell lines after serum exposure)	2.0-fold	.007
	Downregulation	VEGF_HUVEC_30MIN-UP (upregulated 30 minutes after VEGF treatment in human umbilical vein endothelial cells)	1.7-fold	.01

[a]Potentially relevant enriched subsets that were upregulated or downregulated in a statistically significant manner in nodular-enhancing bevacizumab-evasive gliomas (NEBEGs) and in infiltrating bevacizumab-evasive gliomas (IBEGs) are shown.

TABLE 2. Specific Transcripts That Were Upregulated or Downregulated in a Statistically Significant Manner in Bevacizumab-Evasive Gliomas[a]

BEG Subset	Direction of Change	Transcript	Change	*P*
IBEGs	Upregulation	Receptor tyrosine kinase Ephrin A4	2.3-fold	.008
		Matrix metalloproteinase-7	2.3-fold	.009
		Basic fibroblast growth factor	2.1-fold	.009
		Matrix-remodeling associated	1.9-fold	.01
		Insulin-like growth factor binding protein 2	2.1-fold	.02
		Receptor tyrosine kinase C-met	2.5-fold	.003
	Downregulation	Vascular endothelial growth factor-B	2.1-fold	.04
NEBEGs	Upregulation	Vascular endothelial growth factor-A	2.2-fold	.004
		Vascular endothelial growth factor-C	2.1-fold	.003
		Aquaporin 4	2.3-fold	.001
		Aquaporin 10	2.2-fold	.002
	Downregulation	Basic fibroblast growth factor	1.9-fold	.03
		Receptor tyrosine kinase Ephrin A4	1.8-fold	.04
		Matrix metalloproteinase-7	1.9-fold	.04

[a]Potentially relevant enriched subsets that were upregulated or downregulated in nodular-enhancing bevacizumab-evasive gliomas (NEBEGs) and infiltrating bevacizumab-evasive gliomas (IBEGs) are shown. Raw *P* values for each were adjusted by controlling the false discovery rate, generating adjusted *P* values. Although none of the > 25 000 microarray transcripts analyzed on microarrays had adjusted values of $P < .05$, several oncologically pertinent transcripts that were candidate mediators for bevacizumab evasion before the analysis was run had raw values of $P < .05$ and are listed above.

NEBEGs. Immunohistochemical analysis showed that IBEGs maintained the hypoxia and reduced vascularity seen after successful bevacizumab treatment, suggesting that they may have relied on invasion to reduce vascular dependence, whereas NEBEGs reacquired the reduced hypoxia and increased vascularity seen before bevacizumab treatment.

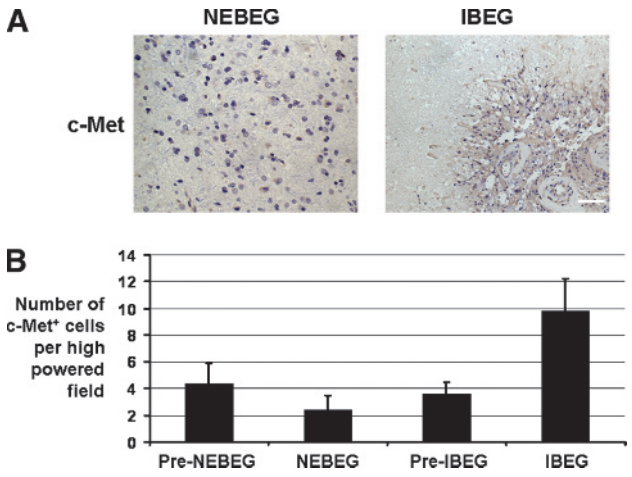

FIGURE 4. C-met immunostaining of bevacizumab-evasive gliomas (BEGs). A, representative c-Met immunostainings of a nodular-enhancing BEG (NEBEG) and an infiltrating BEG (IBEG) are shown. B, the average number of c-Met–positive cells in gliomas before bevacizumab treatment that would go on to become NEBEGs (pre-NEBEGs), NEBEGs, gliomas before bevacizumab treatment that would go on to become IBEGs (pre-IBEGs), and IBEGs are shown, along with standard deviations. Magnification × 100. Scale bar represents 200 μm.

Cluster dendogram analysis confirmed that these radiographic and immunohistochemical differences also were reflected in a microarray analysis. Gene-enrichment subset analysis showed that IBEGs exhibited transcriptional upregulation of gene subsets associated with wound healing, an infiltrative process similar to the infiltration seen in the MRIs of IBEGs, whereas NEBEGs exhibited transcriptional upregulation of gene subsets associated with vascular injury, and the remodeling of blood vessels seen after hypertensive vascular injury may represent an evasive mechanism in NEBEGs. In terms of specific transcripts, IBEGs exhibited increased expression of several invasion-mediating factors. In particular, ephrin A4 promotes basic fibroblast growth factor–mediated glioblastoma cell migration[8]; basic fibroblast growth factor levels increase in the blood of glioma patients whose tumors develop resistance to AZD2171[3]; insulin-like growth

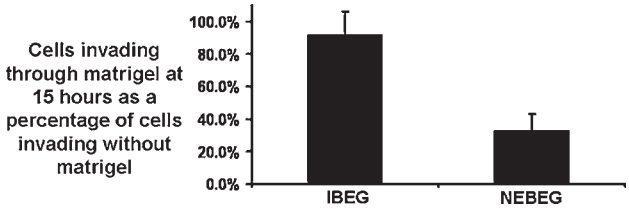

FIGURE 5. Invasiveness of bevacizumab-evasive gliomas (BEGs) assessed in Matrigel chambers. Shown are the number of cells from an IBEG and NEBEG invading through matrigel chambers 15 hours after plating cells taken prospectively from fresh tissue specimens as a percentage of cells invading from the upper to lower wells in control chambers lacking matrigel.

factor binding protein-2 promotes glioma production of the invasion-mediating factor matrix metalloproteinase-2[9]; and C-met promotes glioma migration.[10] On the other hand, NEBEGs exhibited increased VEGF expression compared with before bevacizumab treatment, which could give rise to the increased vascular density and reduced hypoxia seen in our immunohistochemistry of NEBEGs. The functional impact of these distinctions between IBEGs and NEBEGs was confirmed in cells taken from each tumor type, with IBEG cells proving more invasive in Matrigel chambers than NEBEG cells.

Thus, transcriptional upregulation of the factors found in IBEGs could overcome bevacizumab treatment by invasion allowing escape from devascularized areas into areas in closer proximity to blood vessels, giving rise to the subset of bevacizumab-resistant glioblastomas that exhibit an infiltrative radiographic appearance and are not dependent on the nodular-enhancing exponential growth that can no longer be sustained in the setting of VEGF blockade. On the other hand, NEBEGs upregulate factors like VEGF, which may allow NEBEGs to exceed the capacity of bevacizumab-mediated VEGF blockade at the doses given to patients, in turn allowing NEBEGs to reacquire the vascularity and reduced hypoxia they had before bevacizumab treatment. Thus, just as temozolomide, the current standard of care for newly diagnosed glioblastoma, has been shown to create a ''hypermutator'' phenotype associated with glioblastoma recurrence,[11] VEGF-targeted treatments like bevacizumab may cause ''hyperinvasive'' (IBEG) or ''hyperangiogenic'' (NEBEG) phenotypes associated with glioblastoma recurrence. Targeting these phenotypes, perhaps through anti-invasive drugs targeting IBEG-specific factors or VEGF receptor blockers in the case of NEBEGs, will be essential to overcome bevacizumab evasion, a currently untreatable state with rapid mortality. The findings presented here are the first step in the development of treatments for these bevacizumab-evasive human glioblastomas.

Disclosure

This work was supported in part by funding to the laboratory of MKA from the American Brain Tumor Association, the James S. McDonnell Foundation, and the UCSF Brain Tumor SPORE CA097257. The authors have no personal financial or institutional interest in any of the drugs, materials, or devices described in this article.

REFERENCES

1. Vredenburgh JJ, Desjardins A, Herndon JE II, et al. Phase II trial of bevacizumab and irinotecan in recurrent malignant glioma. *Clin Cancer Res*. 2007;13(4):1253-1259.
2. Vredenburgh JJ, Desjardins A, Herndon JE II, et al. Bevacizumab plus irinotecan in recurrent glioblastoma multiforme. *J Clin Oncol*. 2007; 25(30):4722-4729.
3. Batchelor TT, Sorensen AG, di Tomaso E, et al. AZD2171, a pan-VEGF receptor tyrosine kinase inhibitor, normalizes tumor vasculature and alleviates edema in glioblastoma patients. *Cancer Cell*. 2007;11(1):83-95.
4. Kreisl TN, Kim L, Moore K, et al. A phase I trial of enzastaurin in patients with recurrent gliomas. *Clin Cancer Res*. 2009;15(10):3617-3623.
5. Bergers G, Hanahan D. Modes of resistance to anti-angiogenic therapy. *Nat Rev Cancer*. 2008;8(8):592-603.
6. Collins TJ. ImageJ for microscopy. *Biotechniques*. 2007;43(Suppl 1): 25-30.
7. Said HM, Hagemann C, Staab A, et al. Expression patterns of the hypoxia-related genes osteopontin, CA9, erythropoietin, VEGF and HIF-1alpha in human glioma in vitro and in vivo. *Radiother Oncol*. 2007; 83(3):398-405.
8. Fukai J, Yokote H, Yamanaka R, Arao T, Nishio K, Itakura T. EphA4 promotes cell proliferation and migration through a novel EphA4-FGFR1 signaling pathway in the human glioma U251 cell line. *Mol Cancer Ther*. 2008;7(9):2768-2778.
9. Wang H, Shen W, Huang H, et al. Insulin-like growth factor binding protein 2 enhances glioblastoma invasion by activating invasion-enhancing genes. *Cancer Res*. 2003;63(15):4315-4321.
10. Eckerich C, Zapf S, Fillbrandt R, Loges S, Westphal M, Lamszus K. Hypoxia can induce c-Met expression in glioma cells and enhance SF/HGF-induced cell migration. *Int J Cancer*. 2007;121(2):276-283.
11. Hunter C, Smith R, Cahill DP, et al. A hypermutation phenotype and somatic MSH6 mutations in recurrent human malignant gliomas after alkylator chemotherapy. *Cancer Res*. 2006;66(8):3987-3991.

